Radiation Measurements 189 (2025) 107547

Contents lists available at ScienceDirect

Radiation Measurements

journal homepage: www.elsevier.com/locate/radmeas

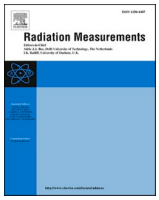

Characterization of low-energy protons by fluorescent nuclear track detectors based on lithium fluoride films on silicon substrates

Massimo Piccinini [a,*], Enrico Nichelatti [b], Valentina Nigro [a], Adriano Zerbini [a], Rosa Maria Montereali [a,1], Concetta Ronsivalle [a], Alessandro Ampollini [a], Maria Aurora Vincenti [a]

[a] ENEA C.R. Frascati, Nuclear Department, Via E. Fermi 45, Frascati, 00044, Rome, Italy
[b] ENEA C.R. Casaccia, Nuclear Department, Via Anguillarese 301, S. Maria di Galeria, 00123, Rome, Italy

ARTICLE INFO

Keywords:
Radiophotoluminescence
Color centers
Thin films
Fluorescent nuclear track detectors
Lithium fluoride
Proton beams

ABSTRACT

In the last years, Fluorescent Nuclear Track Detectors (FNTDs) based on the visible radiophotoluminescence (RPL) of aggregate F_2 and F_3^+ color centers (CCs) in lithium fluoride (LiF) crystals have been demonstrated. On the other hand, optically transparent polycrystalline LiF thin films, grown by thermal evaporation on Si(100) substrates, have been successfully used for proton beam advanced diagnostics, mainly through Bragg curve permanent recording and analysis. In this paper, they were tested as FNTDs for low-energy, nearly monochromatic, collimated proton beams produced by the vertical low-energy extraction line of the TOP-IMPLART proton linear accelerator in operation at ENEA Frascati, Italy. Cleaved LiF films were irradiated with the film plane approximately parallel to the beam propagation direction and the film edge directly exposed to the incident beam. The irradiation caused the formation of CCs along the proton tracks within the film. The luminescent track images were visualized with a fluorescence microscope under blue LED excitation. At the lower energy of ~1 MeV, it was possible to record single entire proton tracks at a fluence of approximately 10^8 protons/cm^2. Their lengths are comparable with those expected in the LiF film. Increasing the proton energy to ~6 MeV, the luminescent tracks were observed mainly close to the expected Bragg peak position, i.e., at the penetration depth where it would be found in Si rather than in LiF, due to multiple Coulomb scattering. At both energies, by raising the fluence by two orders of magnitude, the superposition of a very high number of tracks allowed recording the luminescent Bragg curves of the proton beams in the LiF films. They were analyzed using two different methods, considering also the type of substrate and the film characteristics, allowing to estimate the beam energy spectrum. At ~1 MeV, the Bragg curve was best fitted using a random-optimization approach, while at ~6 MeV it was reproduced using depth-dose curves simulated in FLUKA.

1. Introduction

Lithium fluoride (LiF) is an alkali halide characterized by a face centered cubic structure, which has attracted considerable attention due to its distinctive properties (Montereali and Nalwa, 2002), such as wide optical transparency, chemical and thermal stability and ionic conductivity. The LiF applications in the form of films have significantly broadened over the decades, extending from lithium ion battery (Sharopov et al., 2025) to optics (Li et al., 2025) and electronics (Montereali et al., 2004), where very thin LiF films enhance the contact between the Al electrodes and the organic layers in plastic solar cells and serve as a cathode material with Al in organic light-emitting diodes (OLEDs).

Historically, the sensitivity to high-energy radiation (X-rays, gamma rays) and charged and neutral particles, leading to the formation of color centers (CCs) (Schulman and Compton, 1963; Agullo-Lopez et al., 1988), has made LiF an interesting material for solid-state dosimeters. The concentration of luminescent CCs created by the interaction with ionizing radiation is locally related to the energy absorbed by the material. After irradiation, under suitable light stimulation, the measured

This article is part of a special issue entitled: SSD21 published in Radiation Measurements.

* Corresponding author.
E-mail address: massimo.piccinini@enea.it (M. Piccinini).
[1] Current address: Via A. Cassani 39, 00046, Grottaferrata (Rome), Italy.

https://doi.org/10.1016/j.radmeas.2025.107547
Received 7 August 2025; Received in revised form 19 September 2025; Accepted 27 October 2025
Available online 27 October 2025

visible radiophotoluminescence (RPL) intensity is proportional to the integrated radiation dose released in the material (Levita and Schlesinger, 1976). Currently, the sensitivity of this technique allowed the measurements of dose values typical of radiotherapy (Piccinini et al., 2022; Villarreal-Barajas et al., 2015), even in thin films (Kurobori and Matoba, 2014; Vincenti et al., 2023). Heavily irradiated LiF crystals were also utilized as active media in optically pumped tunable lasers operating in the visible and near-infrared range at room temperature (Basiev et al., 1988), as well as in miniaturized light-emitting photonic devices (Montereali et al., 2025), also in the form of thin films (Montereali and Nalwa, 2002). Two decades ago, very high-spatial resolution soft X-ray imaging detectors based on the visible RPL of CCs in LiF crystals and thermally evaporated thin films were proposed by our group (Baldacchini et al., 2003) for contact soft X-ray microscopy. Their use was extended to higher X-ray energies (Montereali et al., 2023a), thanks to their peculiarities and versatility and to the characterization of intense X-ray sources even in extreme conditions (Bonfigli Capotondi et al., 2019). In the last decade, the imaging capabilities of these radiation detectors have been successfully used for proton beam diagnostics (Piccinini et al., 2014, 2017), mainly through full Bragg curve permanent recording and analysis in LiF crystals (Nichelatti et al., 2017; Piccinini et al., 2019), which allow an accurate determination of the beam energy and energy spread, and in LiF films (Nichelatti et al., 2022; Montereali et al., 2023b).

In the last years, nominally pure LiF single crystals were proposed as Fluorescent Nuclear Track Detectors (FNTDs) for detecting alpha particles (Bilski and Marczewska, 2017; Bilski et al., 2017; Sankowska et al., 2022), fast and thermal neutrons (Bilski et al., 2018), as well as heavier ions (Bilski et al., 2019a, 2019b). Only recently, the investigation of LiF crystals for the detection of protons tracks has been reported at high energies (Bilski et al., 2024) and by our group at lower energies (<3 MeV) (Nichelatti et al., 2025a; Piccinini et al., 2024b) and, for the first time, also in LiF thin films at 1 MeV (Piccinini et al., 2025). At this energy, the optically transparent LiF films grown on Si(100), after substrate cleavage, appears suitable for both full Bragg curve and single proton tracks recording for irradiation parallel to the substrate. It should be noted that this convenient geometry does not allow recording of entire fluorescent tracks for proton energies <2 MeV in LiF crystals because of their limited penetration, which implies that they are mainly covered by the intense light scattering at the crystal edge. Moreover, the choice of the reflective silicon substrate was demonstrated to be an advantage for the RPL enhancement, up to 50 % with respect to glass one (Vincenti et al., 2021). In the fluorescence images, the reduction of the background due to the limited thickness of the LiF film improves image contrast, which is critical for single track recording (Piccinini et al., 2025). Apart from the easier cleavage, the oriented Si(100) substrate assures good homogeneity, reproducibility and compactness for the LiF films thermally evaporated in controlled growth conditions (Vincenti et al., 2021).

Currently, nominally pure LiF crystals are considered suitable materials for radiation dosimetry based on RPL for FNTD realization (Christensen et al., 2024) together with the well-assessed Al_2O_3:C, Mg crystals (Akselrod et al., 2006; Akselrod and Sykora, 2011; Akselrod and Kouwenberg, 2018) and Ag-doped phosphate glass (Kurobori et al., 2017; Kodaira et al., 2020).

These novel FNTDs are based on the aggregate F_2 and F_3^+ CCs (two electrons bound to two and three anion vacancies, respectively), stable at room temperature, whose overlapping absorption bands are centered around 450 nm, generally known as the M band (Nahum and Wiegand, 1967). The RPL spectrum, obtained by optical excitation in the M band, exhibits two Stokes-shifted broad emission bands peaking at about 678 nm and 541 nm, corresponding to the F_2 and F_3^+ emission bands, respectively (Baldacchini et al., 2000; Piccinini et al., 2025). In this paper, optically transparent polycrystalline LiF films, thermally evaporated on reflective Si(100) substrates, were tested as FNTD at the proton energies of ~1 and ~6 MeV, with the aim of studying their behavior and better understanding the role of the used substrate in the observed fluorescent individual tracks and Bragg curves at energies of interest for radiobiology experiments.

2. Materials and methods

Optically transparent LiF films, between 1 and 2 μm thick, were grown at ENEA Frascati (Italy) by thermal evaporation on 0.5 mm thick Si(100) substrates, constantly kept at a temperature of 300 °C during deposition (Leoncini et al., 2019), performed in a vacuum chamber at a pressure below 1 mPa with a controlled deposition rate of 1 nm/s. More details can be found in (Vincenti et al., 2021). Their optical characterization was performed by means of ellipsometric spectral measurements with a Woollam VASE instrument, and subsequently analyzed with the open-source software KSEMAW (Montecchi et al., 2023) for the film of lower thickness. For the thickest LiF film the optical reflectivity spectrum was measured by a PerkinElmer Lambda 1050+ spectrophotometer at near-normal incidence. Its refractive index dispersions in the visible range and other important features (thickness, surface roughness, material packing density, etc.) were estimated by a best fit with a model that allows taking into account spectral changes due to film deviations from the ideally perfect thin-film model (Montecchi et al., 2001), developed in Matlab (The MathWorks and Inc, 2010).

The films, cleaved into two halves, were irradiated with the film surface approximately parallel to the beam propagation axis (edge-on irradiation) and the cleaved film edge directly exposed to the incident, nearly monochromatic, collimated pulsed proton beam delivered by the vertical low-energy extraction beamline of the TOP-IMPLART linear accelerator operating at ENEA Frascati (Picardi et al., 2020). The protons are produced by a commercial linac, the PL7 injector manufactured by ACCSYS-HITACHI, followed by a 90° dipole bending the beam into the 80 cm long vertical extraction beamline. The injector consists in a sequence of two accelerators, a RFQ with a maximum energy of 3 MeV and a DTL with a maximum energy of 7 MeV. Intermediate energies can be produced by adjusting the amplitude of the accelerating field and the proton energy at the injector exit is retrieved by the value of the current in the coils of the bending magnet. After the beam is bent, the pristine energy from the injector is degraded due to the passage of the protons through a 2 μm-thick gold foil followed by a 2 mm-diameter collimator (to obtain a round homogeneous irradiation spot on the target), a 50 μm-thick Kapton window separating the vacuum from air and a path in air whose thickness depends on the distance of the sample from the exit window, typically 25 mm. The final beam energy on the target at the end of the vertical beamline in air varies between 1 and 6.5 MeV, with fluence adjustable over several orders of magnitude.

The proton beam and track images were acquired using a Nikon Eclipse 80i fluorescence microscope, equipped with 20 × and 100 × objectives and a 440 nm pE-100 coolLED source for exciting the RPL of CCs. Emission was selected by a Chroma AT515lp filter and detected with an Andor NEO sCMOS camera operating at 16-bit, with acquisition times between 75 and 150 s. The acquired images were processed using ImageJ software (ImageJ) to extract the profile of the luminescent Bragg curves stored in the films irradiated at high fluences. In order to estimate the energy spectrum of the proton beams, at ~1 MeV, the experimental Bragg curve was best fitted using a recently developed procedure (Nichelatti et al., 2025b) consisting in a random-optimization approach, where Bragg curves in LiF are calculated using a smart interpolation of a set of Monte Carlo simulated Bragg curves of monochromatic protons while varying the number of energy bins during the random-optimization cycles to increase the energy spectral resolution. At ~6 MeV, contrary to the case of ~1 MeV, due to multiple Coulomb scattering (MCS), proton leakage from the film and migration from the substrate into the film cannot be neglected (Montereali et al., 2023b), so the Bragg curve was reproduced using the Monte Carlo software FLUKA, version 4–5.0 (Website: https; Battistoni et al., 2015; Ahdida et al., 2022), in combination with its graphical user interface Flair, version

3.4–1 (Donadon et al., 2024).

3. Results and discussion

The edge-on irradiation of the LiF films on Si was performed choosing a suitable fluence value to ensure non-superimposed proton tracks. At the energy of ~1 MeV, the pulsed beam from the accelerator was set at a charge of 0.5 pC/pulse and 50 beam pulses were delivered to the sample. By irradiating a LiF crystal with its surface perpendicular to the beam propagation axis, we could estimate a fluence of approximately 10^8 protons/cm^2 (Piccinini et al., 2024b). Fig. 1 shows the fluorescence image of the proton tracks in a LiF film recorded with a good signal-to-noise ratio, by exploiting the enhancement of the visible RPL due to the presence of the reflecting Si substrate (Vincenti et al., 2021), along with the reduction of the background due to the limited thickness of the LiF film, irradiated under these conditions. The tracks at the edge of the film are approximately 15 μm in length with a minimum lateral separation of ~1 μm; however, at distances larger than 15 μm, some fluorescent tracks could be detected due to protons that did not directly enter the film through its edge, rather through its surface as a consequence of a very small angular tilt of the sample, that exposed the entire film surface directly to grazing-incident protons. To characterize the energy spectrum of the proton beam, another cleaved LiF film sample was irradiated by delivering 3750 pulses, corresponding to an increased fluence by two orders of magnitude. Under these conditions, the high proton fluence prevented the recording of individual tracks, because they resulted totally superimposed, as shown in the left picture of Fig. 2. By integrating the entire image along the direction parallel to the film edge, the RPL depth profile (experimental Bragg curve) of the proton beam was obtained (see Fig. 2, right). For the irradiation of LiF films, thermally evaporated on glass substrates, with protons at nominal energies of 3 and 7 MeV and within a range of doses from 10^3 up to 10^7 Gy, it was experimentally observed that the RPL intensity of F_2 and F_3^+ CCs increases linearly with dose until saturation is reached at the highest values, and that the RPL intensity does not depend on Linear Energy Transfer (LET) (Piccinini et al., 2015). An elementary model, based on radiation-mediated creation and annihilation of CCs, was developed to describe this behavior (Piccinini et al., 2017).

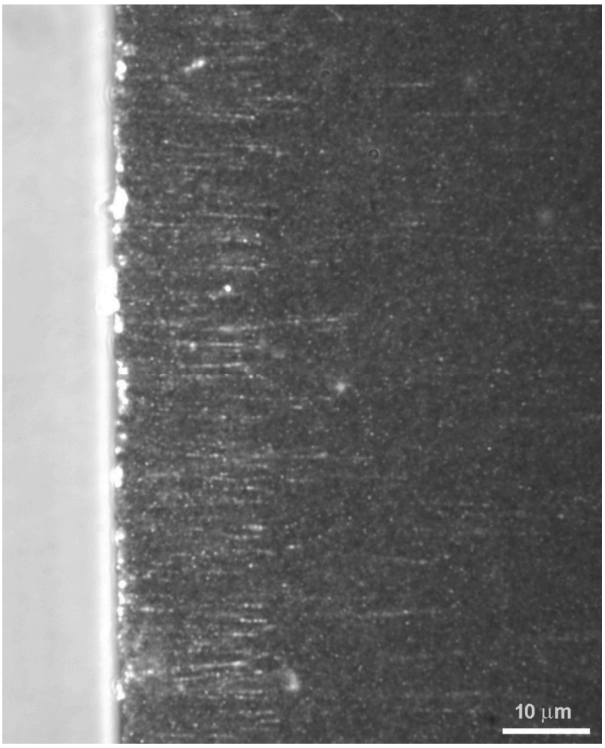

Fig. 1. Fluorescent proton tracks recorded in a 1.18 μm-thick LiF film thermally evaporated on Si(100) and irradiated with a ~1 MeV beam impinging from the left on the cleaved film edge at a fluence of 10^8 protons/cm^2.

A recently developed fitting procedure (Nichelatti et al., 2025b) was applied to the RPL depth profile shown on the right of Fig. 2, to estimate the energy spectrum of the proton beam responsible for the formation of F_2 and F_3^+ CCs in the LiF film. This film, approximately 1 μm thick, was characterized by means of ellipsometry; by comparing the measured refractive index in the visible with tabulated values for LiF (Palik, 1991), we estimated a material packing density of approximately 88.6 %. Although it has been demonstrated that in thin films MCS causes beam protons that have penetrated the underlying substrate to migrate into the film – becoming the main source of energy deposition in it and shifting the luminescent Bragg peak accordingly – and that some protons entering the film progressively leak out, these effects are considered negligible at energies ~1 MeV for film thicknesses of 1 μm or more (Montereali et al., 2023b). Since a preliminary analysis indicated that the peak energy of the beam was ~1 MeV, we were able to apply the aforementioned fitting procedure – originally developed for bulk LiF – to analyze the RPL depth profile detected in the film. In this procedure, the increased proton penetration range in the LiF film, due to its lower material density compared to bulk LiF (Knoll, 2010; Nichelatti et al., 2019), was considered. The fitting procedure, implemented in Matlab (The MathWorks and Inc, 2010), relies on the reasonable assumption that the Bragg curve of a polychromatic proton beam can be modeled as a weighted superposition of Bragg curves generated by monochromatic beams. The weights of these monochromatic components can, in principle, be determined using any optimization method. In our case, following a recently published approach (Nichelatti et al., 2025b), we employed a random-optimization algorithm to determine the areas of a discrete set of energy bins spanning a defined energy range. These bins are designed to represent the energy spectrum in the form of a histogram. The bin widths were selected to be sufficiently narrow to approximate the monochromatic components of the energy spectrum.

At each step of the optimization, the bin heights are randomly modified within predefined limits. The resulting total Bragg curve – obtained as a weighted superposition of individual monochromatic Bragg curves, each previously simulated in FLUKA to construct a Bragg-curve LUT – is then compared with the experimental luminescent Bragg curve. Based on this comparison, the corresponding energy spectrum is either accepted or rejected and another optimization step is performed (Nichelatti et al., 2025b). At the end of the process, the energy spectrum is slightly shifted and rescaled to account for the packing density of the film, as described in (Nichelatti, 2025). In the present paper, the method was applied by sampling the energy range from 280 keV to 1.77 MeV using 50 equally spaced bins, each with a width of 29.8 keV. The resulting spectral distribution exhibits a main peak centered at approximately 1.10 MeV, with a full width at half maximum (FWHM) of about 183 keV.

A second set of irradiations was performed by setting the accelerator at a beam energy of ~6 MeV with a charge of 2 pC/pulse. After edge-on irradiating a LiF film with 50 pulses, the image of proton tracks was acquired using the fluorescence microscope. The image is shown in Fig. 3, together with enlarged views of three regions. Due to four-time higher charge per pulse (estimated fluence of ~4 × 10^8 protons/cm^2), with respect to the ~1 MeV case, some track superpositions are observed. These are also ascribable to scattered much longer proton trajectories, with a lateral separation <1 μm among the tracks. At the energy of ~1 MeV, due to the short proton penetration depth and LET in the range from 50 to 130 keV/μm, entire tracks are observed. Increasing the proton energy to ~6 MeV, due to the lower LET in the range from 15 to 70 keV/μm, the luminescent tracks are observed with a good signal-to-noise ratio mainly close to the Bragg peak position. Again, by increasing the fluence by two orders of magnitude, the superposition of a very high number of tracks allowed recording the experimental RPL

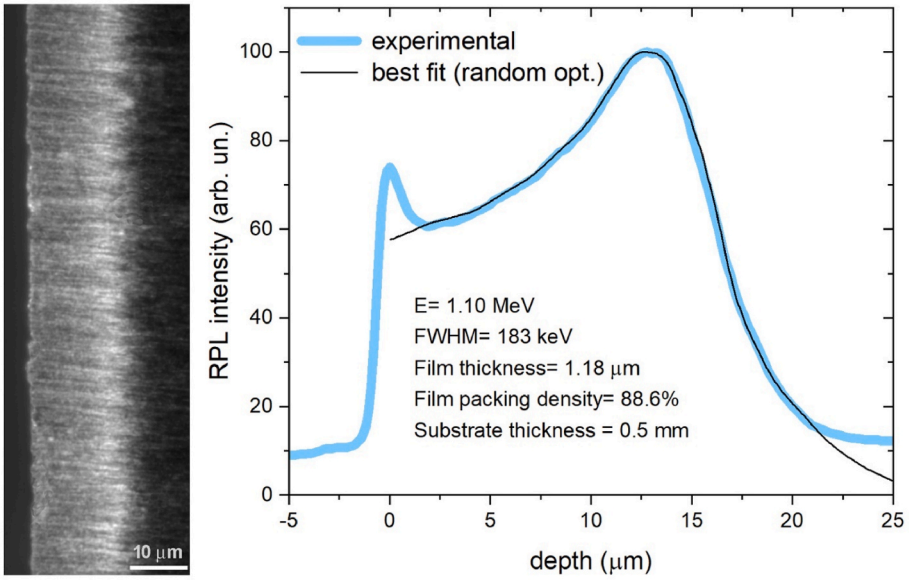

Fig. 2. *Left:* Fluorescent proton tracks recorded in a 1.18 μm-thick LiF film thermally evaporated on Si(100) and irradiated with a ~1 MeV beam impinging from the left on the cleaved film edge at a fluence of $\sim 10^{10}$ protons/cm^2; *Right:* Experimental RPL profile of the Bragg curve obtained by integrating along the direction parallel to the film edge the picture on the left and its best-fitting curve obtained by using the random-optimization approach (see text for details).

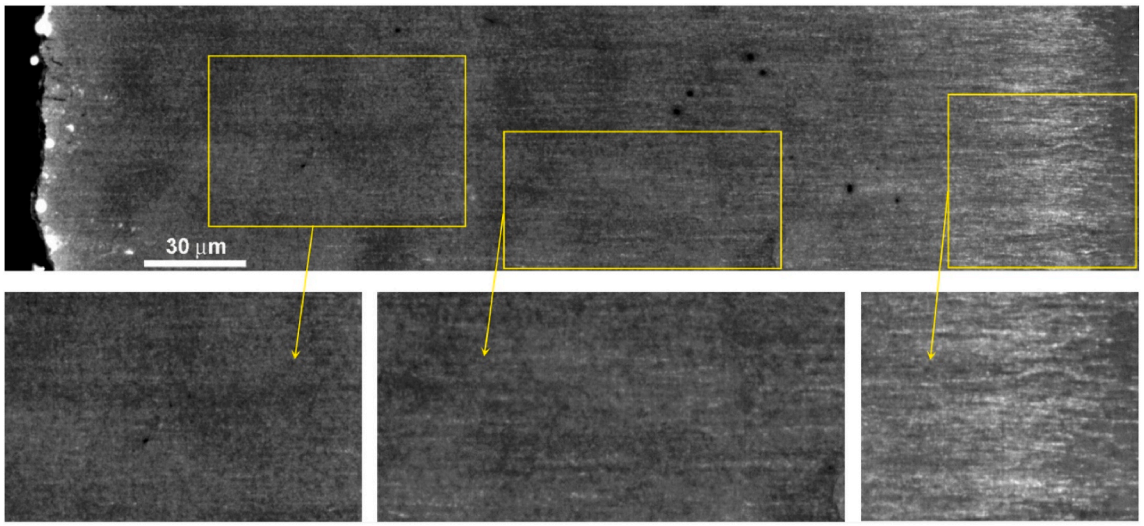

Fig. 3. *Top:* Fluorescent proton tracks recorded in a 2.23 μm-thick LiF film thermally evaporated on Si(100) and irradiated with a ~6 MeV beam impinging from the left on the cleaved film edge at a fluence of 4×10^8 protons/cm^2; *Bottom:* enlarged views of three regions.

depth profile of the proton beam, after integrating the entire image shown on the left in Fig. 4 along the direction parallel to the film edge (see Fig. 5).

In contrast to the sample irradiated with protons of energy ~1 MeV, the RPL depth profile presented in Fig. 5 could not be analyzed using the fitting procedure introduced in (Nichelatti et al., 2025b). Indeed, as suggested by the Bragg peak located at approximately 300 μm depth, the energy of the proton beam was estimated to be sufficiently high – around 6 MeV – to induce non-negligible proton migration from the substrate into the film due to MCS, resulting in a shift of the luminescent Bragg peak and an overall deformation of the Bragg curve, as discussed in (Montereali et al., 2023b). For this reason, the analysis of this sample was instead carried out by replicating the measured RPL depth profile with a simulated energy deposition profile, under the assumption that the RPL intensity is locally proportional to the energy deposited by protons in the material (Piccinini et al., 2023, 2024a). To this end, energy deposition simulations were performed using the Monte Carlo code FLUKA. The simulated sample geometry included a LiF film with thickness of 2.23 μm and a packing density of 96 %, as estimated from the analysis of the sample optical reflectivity spectrum measured in the visible range. Simulations reported in (Montereali et al., 2023b) show that the packing density does not have significant effects at these energies, where MCS from the Si substrate dominates. On the other hand, the film thickness influences the shaping of the Bragg curve and it is properly considered in the simulations. The simulated proton beam, with a transverse size of 2 mm, was collimated and vertically centered 250 μm below the interface between the Si substrate and the LiF film. The vertical y-axis was defined such that $y = 0$ corresponds to this interface between the two materials (see the bottom-right picture in Fig. 4). The origin of the z-axis (penetration depth) was set at the sample edge. The horizontal x-axis was defined as the direction parallel to the film edge and coincident with the film edge itself. Other simulation parameters included the launch of 2.5×10^7 virtual protons, and the *Ekin Frac* parameter of the FLUKAFIX card set to 0.01 for both the LiF

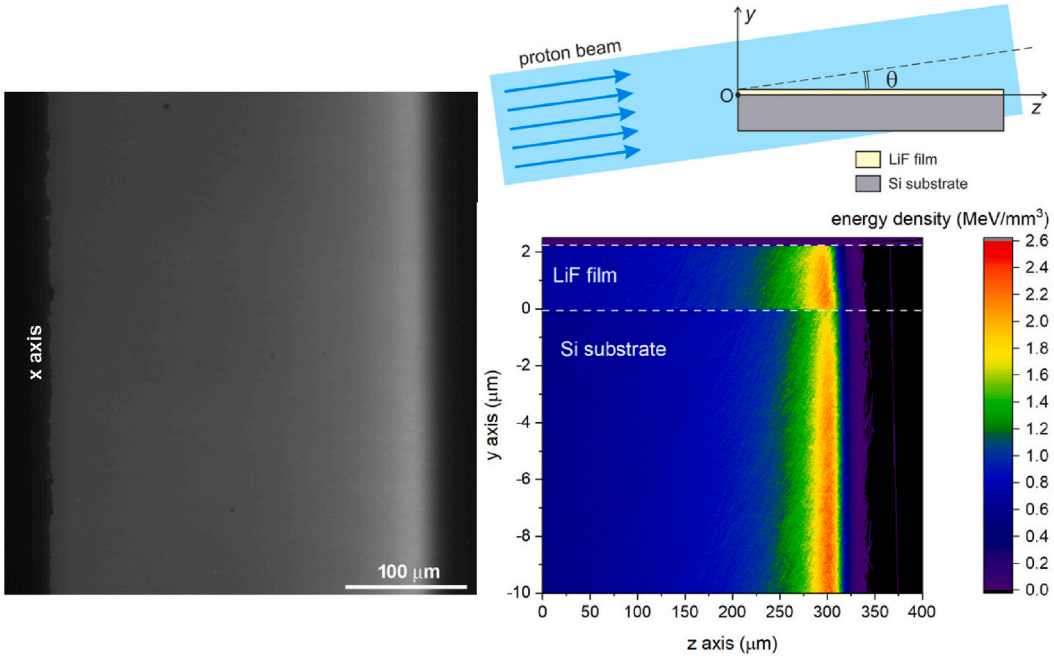

Fig. 4. *Left:* Fluorescent image of proton tracks recorded in a 2.23 μm-thick LiF film thermally evaporated on Si(100) and irradiated with a ~6 MeV beam impinging from the left on the cleaved film edge at a fluence of $\sim 10^{10}$ protons/cm^2; *Upper right*: Scheme of the irradiation geometry; *Lower right*: Energy deposited by the proton beam in the LiF film and in the Si substrate as a function of proton penetration depth (*z*-axis), as simulated using FLUKA (*x*-average, transverse view).

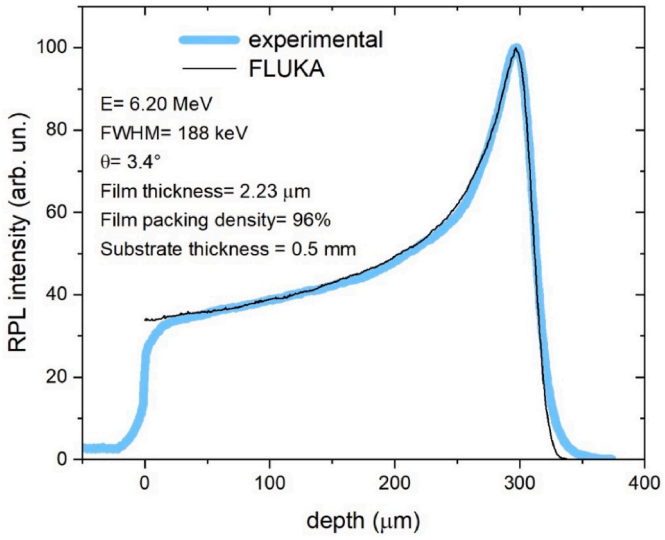

Fig. 5. Experimental RPL profile of the Bragg curve obtained by integrating along the *x*-axis the left picture of Fig. 4 and its best-matching curve simulated in FLUKA.

and Si materials. Energy deposition was scored using the USRBIN card within a volume defined by -5 mm $\leq x \leq 5$ mm (100 sampled points), -10 μm $\leq y \leq 2.5$ μm (625 sampled points), and $0 \leq z \leq 400$ μm (800 sampled points). Among the various simulation configurations tested, the ones that best reproduced the experimental RPL depth profile corresponded to a Gaussian energy spectrum with a mean energy of 6.20 MeV a and FWHM of 188 keV (i.e., a standard deviation of 80 keV). The best match was obtained assuming a grazing incidence angle of 3.4° for the proton beam, as if the beam were impinging from the half-space facing the substrate – see the upper-right picture in Fig. 4 for a schematic representation of this tilted irradiation geometry.

4. Conclusions

Optically transparent, uniform, polycrystalline LiF thin films, grown on Si(100) substrates by thermal evaporation, have been tested as FNTDs for collimated proton beams of energies of ~1 and ~6 MeV. The irradiation causes the local formation of stable CCs in the crystal lattice, among them the F_2 and F_3^+ ones, which show efficient visible photoluminescence in the red and green spectral ranges, respectively, under blue light simultaneous excitation. The cleaved LiF films were irradiated approximately parallel to the proton beam at fluence values between 1 and 4 × 10^8 protons/cm^2. At the energy of ~1 MeV, due to the short proton penetration depth and high LET, entire tracks were observed with a good signal-to-noise ratio. Increasing the proton energy to ~6 MeV, due to lower LET, the luminescent tracks were observed mainly close to the Bragg peak, whose depth is where it would be found in Si rather than in LiF, due to MCS. By increasing fluence by two orders of magnitude, the superposition of a very high number of tracks allowed recording the luminescent Bragg curve of the proton beams. The beam average energy and energy spread were obtained by fitting such experimental profiles using a random-optimization approach at ~1 MeV and using depth-dose curves simulated in FLUKA at ~6 MeV, by properly considering the film characteristics and the substrate. Although the intensity and contrast along a single track is not enough to obtain the proton energy deposition profile, as observed also in LiF crystals FNTD (Piccinini et al., 2024b) in similar conditions, the advanced proton beam characterization performed through the Bragg curve RPL profiles at high fluences confirms an intrinsic LET independence, despite the high ionization density in the core of the low-energy proton tracks. It should be noted that the recording of both the entire proton tracks and the fluorescent Bragg curve for proton energies <2 MeV is prevented in LiF crystals because of their limited penetration, which implies that they are mainly covered by the intense light scattering at the crystal edge. Moreover, the choice of the reflective silicon substrate has the advantage of visible RPL response enhancement, up to 50 % with respect to the glass one (Vincenti et al., 2021). In the fluorescence images, the reduction of the background due to the limited thickness of the LiF film improves the image contrast, which is critical for single track recording

(Piccinini et al., 2025). Apart from the easier cleavage, the oriented Si (100) substrate assures a good homogeneity, reproducibility and compactness for the LiF films thermally evaporated in controlled growth conditions (Vincenti et al., 2021). Then the ability in the growth of optically transparent LiF thin films on a reflective substrate like silicon allows for fluorescent single proton tracks observation, as well as for low-energy proton beam characterization from entire Bragg curve recording and analysis. Further experiments are in progress to better understand the potential improvement of this technology for future developments in radiobiology.

CRediT authorship contribution statement

Massimo Piccinini: Writing – review & editing, Writing – original draft, Validation, Methodology, Investigation, Formal analysis, Data curation, Conceptualization. **Enrico Nichelatti:** Writing – review & editing, Writing – original draft, Validation, Software, Methodology, Investigation, Formal analysis, Data curation, Conceptualization. **Valentina Nigro:** Writing – review & editing, Methodology, Conceptualization. **Adriano Zerbini:** Methodology, Investigation. **Rosa Maria Montereali:** Writing – review & editing, Writing – original draft, Resources, Methodology, Conceptualization. **Concetta Ronsivalle:** Writing – review & editing, Supervision, Methodology, Conceptualization. **Alessandro Ampollini:** Methodology, Investigation. **Maria Aurora Vincenti:** Writing – review & editing, Supervision, Methodology, Conceptualization.

Declaration of competing interest

The authors declare that they have no known competing financial interests or personal relationships that could have appeared to influence the work reported in this paper.

Acknowledgements

The authors would like to thank F. Menchini and M. Montecchi for providing the ellipsometric characterization of the LiF films and E. Cisbani, C. De Angelis and G. Esposito for their valuable suggestions and discussions.

Data availability

Data will be made available on request.

References

Agullo-Lopez, F., Catlow, C.R.A., Townsend, P.D., 1988. Point Defects in Materials. Academic, London.

Ahdida, C., Bozzato, D., Calzolari, D., Cerutti, F., Charitonidis, N., Cimmino, A., Coronetti, A., D'Alessandro, G.L., Donadon Servelle, A., Esposito, L.S., Froeschl, R., García Alía, R., Gerbershagen, A., Gilardoni, S., Horváth, D., Hugo, G., Infantino, A., Kouskoura, V., Lechner, A., Lefebvre, B., Lerner, G., Magistris, M., Manousos, A., Moryc, G., Ogallar Ruiz, F., Pozzi, F., Prelipcean, D., Roesler, S., Rossi, R., Sabaté Gilarte, M., Salvat Pujol, F., Schoofs, P., Stránský, V., Theis, C., Tsinganis, A., Versaci, R., Vlachoudis, V., Waets, A., Widorski, M., 2022. New capabilities of the FLUKA multi-purpose code. Front. Physiol. 9, 788523.

Akselrod, M., Kouwenberg, J., 2018. Fluorescent nuclear track detectors – review of past, present and future of the technology. Radiat. Meas. 117, 35.

Akselrod, M.S., Sykora, G.J., 2011. Fluorescent nuclear track detector technology—a new way to do passive solid state dosimetry. Radiat. Meas. 46, 1671.

Akselrod, G.M., Akselrod, M.S., Benton, E.R., Yasuda, N., 2006. *A novel Al_2O_3 fluorescent nuclear track detector for heavy charged particles and neutrons*. Nucl. Instrum. Methods Phys. Res. B 247, 295.

Baldacchini, G., De Nicola, E., Montereali, R.M., Scacco, A., Kalinov, V., 2000. Optical Bands of F_2 and F3+ centers in LiF. J. Phys. Chem. Solid. 61, 21.

Baldacchini, G., Bonfigli, F., Faenov, A., Flora, F., Montereali, R.M., Pace, A., Pikuz, T., Reale, L., 2003. Lithium fluoride as a novel X-Ray image detector for biological μ-World capture. J. Nanosci. Nanotechnol. 3 (6), 483.

Basiev, T.T., Mirov, S.B., Osiko, V.V., 1988. Room-temperature color center lasers. IEEE J. Quant. Electron. 24, 1052.

Battistoni, G., Boehlen, T., Cerutti, F., Chin, P.W., Esposito, L.S., Fassò, A., Ferrari, A., Lechner, A., Empl, A., Mairani, A., Mereghetti, A., Garcia Ortega, P., Ranft, J., Roesler, S., Sala, P.R., Vlachoudis, V., Smirnov, G., 2015. Overview of the FLUKA code. Ann. Nucl. Energy 82, 10.

Bilski, P., Marczewska, B., 2017. Fluorescent detection of single tracks of alpha particles using lithium fluoride crystals. Nucl. Instrum. Methods Phys. Res. B 392, 41.

Bilski, P., Marczewska, B., Gieszczyk, W., Kłosowski, M., Nowak, T., Naruszewicz, M., 2017. Lithium fluoride crystals as fluorescent nuclear track detectors. Radiat. Protect. Dosim. 178, 1.

Bilski, P., Marczewska, B., Kłosowski, M., Gieszczyk, W., Naruszewicz, M., 2018. Detection of neutrons with LiF fluorescent nuclear track detectors. Radiat. Meas. 116, 35.

Bilski, P., Marczewska, B., Gieszczyk, W., Kłosowski, M., Naruszewicz, M., Zhydachevskyy, Y., Sankowska, M., Kodaira, S., 2019a. Fluorescent imaging of heavy charged particle tracks with LiF single crystals. J. Lumin. 213, 82.

Bilski, P., Marczewska, B., Gieszczyk, W., Kłosowski, M., Naruszewicz, M., Zhydachevskyy, Y., Kodaira, S., 2019b. Luminescent properties of LiF crystals for fluorescent imaging of nuclear particle tracks. Opt. Mater. 90, 1.

Bilski, P., Marczewska, B., Sankowska, M., Kilian, A., Swakoń, J., Siketić, Z., Olko, P., 2024. Detection of proton tracks with LiF fluorescent nuclear track detectors. Radiat. Meas. 173, 107083.

F. Bonfigli, on behalf of F. Capotondi et al, Imaging detectors based on photoluminescence of radiation-induced defects in lithium fluoride for XFEL beam monitoring, Il Nuovo Cimento 42 C (2019) 237.

Christensen, J.B., Muñoz, I.D., Bilski, P., Conte, V., Olko, P., Bossin, L., Vestergaard, A., Agosteo, S., Rosenfeld, A., Tran, L., Knežević, Ž., Majer, M., Ambrožová, I., Parisi, A., Gehrke, T., Martišíková, M., Bassler, N., 2024. Status of LET assessment with active and passive detectors in ion beams. Radiat. Meas. 177, 107252.

Donadon, A., Hugo, G., Theis, C., Vlachoudis, V., 2024. FLAIR3 – recasting simulation experiences with the advanced interface for FLUKA and other Monte Carlo codes. EPJ Web Conf. 302. SNA + MC 2024).

ImageJ (*Image Processing and analysis in Java*). Available online: https://imagej.net/ij/index.html.

Knoll, G.F., 2010. Radiation Detection and Measurement. John Wiley & Sons, New York, NY.

Kodaira, S., Kusumoto, T., Kitamura, H., Yanagida, Y., Koguchi, Y., 2020. *Characteristics of fluorescent nuclear track detection with Ag^+-activated phosphate glass*. Radiat. Meas. 132, 106252.

Kurobori, T., Matoba, A., 2014. Development of accurate two-dimensional dose-imaging detectors using atomic-scale color centers in Ag-activated phosphate glass and LiF thin films. Jpn. J. Appl. Phys. 53, 02BD14.

Kurobori, T., Yanagida, Y., Kodaira, S., Shirao, T., 2017. Fluorescent nuclear track images of Ag-activated phosphate glass irradiated with photons and heavy charged particles. Nucl. Instrum. Methods Phys. Res. 855, 25.

Leoncini, M., Vincenti, M.A., Bonfigli, F., Libera, S., Nichelatti, E., Piccinini, M., Ampollini, A., Picardi, L., Ronsivalle, C., Mancini, A., Rufoloni, A., Montereali, R.M., 2019. Optical investigation of radiation-induced color centers in lithium fluoride thin films for low-energy proton-beam detectors. Opt. Mater. 88, 580.

Levita, M., Schlesinger, T., 1976. LiF dosimetry based on radiophotoluminescence (RPL). IEEE Trans. Nucl. Sci. 23, 667.

Li, S., Honrado-Benítez, C., López-Reyes, P., Larruquert, J.I., Zhang, J., Wang, Z., 2025. Self-consistent optical constants of LiF films. Opt. Express 33 (13), 27716.

Montecchi, M., Montereali, R.M., Nichelatti, E., 2001. Reflectance and transmittance of a slightly inhomogeneous thin film bounded by rough, unparallel interfaces. Thin Solid Films 396, 262.

Montecchi, M., Mittiga, A., Malerba, C., Menchini, F., 2023. KSEMAW: an open source software for the analysis of spectrophotometric, ellipsometric and photothermal deflection spectroscopy measurement. Open Res. Eur. 1, 95.

Montereali, R.M., 2002. In: Nalwa, H.S. (Ed.), Handbook of Thin Film Materials, vol. 3. Academic, S. Diego, p. 399 ch.7.

Montereali, R.M., Gambino, S., Loreti, S., Gagliardi, S., Pace, A., Baldacchini, G., Michelotti, F., 2004. Morphological, electrical and optical properties of organic light-emitting diodes with a LiF/Al cathode and an Al-Hydroxyquinoline/Diamine junction. Synth. Met. 143, 171.

Montereali, R.M., Bonfigli, F., Nichelatti, E., Piccinini, M., Vincenti, M.A., 2023a. 2.3 Luminescence of point defects in lithium fluoride thin layers for radiation imaging detectors at the nanoscale. In: Meixner, A.J., Fleischer, M., Kern, D.P., Sheremet, E., McMillan, N. (Eds.), Optical NanoSpectroscopy, Volume 3: Applications. De Gruyter, Berlin, Boston, pp. 69–96.

Montereali, R.M., Nigro, V., Piccinini, M., Vincenti, M.A., Ampollini, A., Nenzi, P., Ronsivalle, C., Nichelatti, E., 2023b. Bragg curve detection of low-energy protons by radiophotoluminescence imaging in lithium fluoride thin films. Sensors 23, 4779.

Montereali, R.M., Mussi, V., Nichelatti, E., Piccinini, M., 2025. Photonics in wide-band-gap materials: the challenge of color-center waveguides in lithium fluoride. Opt. Mater. 160, 116719.

Nahum, J., Wiegand, D.A., 1967. Optical properties of some F -Aggregate centers in LiF. Phys. Rev. 154, 817.

Nichelatti, E., 2025. Energy spectrum and Bragg curve of a proton beam in low-density lithium fluoride. ENEA Technical Report. https://doi.org/10.13140/RG.2.2.26839.53929. RT/2025/14/ENEA, ISSN/2499-5347.

Nichelatti, E., Piccinini, M., Ampollini, A., Picardi, L., Ronsivalle, C., Bonfigli, F., Vincenti, M.A., Montereali, R.M., 2017. Bragg-curve imaging of 7 MeV protons in a lithium fluoride crystal by fluorescence microscopy of colour centres. Europhys. Lett. 120, 56003.

Nichelatti, E., Ronsivalle, C., Piccinini, M., Picardi, L., Montereali, R.M., 2019. An analytical approximation of proton Bragg curves in lithium fluoride for beam energy distribution analysis. Nucl. Instrum. Methods Phys. Res. B 446, 29.

Nichelatti, E., Nigro, V., Piccinini, M., Vincenti, M.A., Ampollini, A., Picardi, L., Ronsivalle, C., Montereali, R.M., 2022. Photoluminescent Bragg curves in lithium fluoride thin films on silicon substrates irradiated with a 35 MeV proton beam. J. Appl. Phys. 132, 014501.

Nichelatti, E., Piccinini, M., Ampollini, A., Anello, P., Astorino, M.D., Bazzano, G., Cisbani, E., De Angelis, C., Esposito, G., Limosani, F., Nenzi, P., Nigro, V., Ronsivalle, C., Santavenere, F., Surrenti, V., Trinca, E., Vincenti, M.A., Montereali, R. M., 2025a. Energy spectrum of protons below 10 MeV using color-center radiophotoluminescence in LiF crystals: a Monte Carlo-supported random-optimization estimator. Nucl. Instrum. Methods Phys. Res. 1072, 170218.

Nichelatti, E., Piccinini, M., Ampollini, A., Anello, P., Astorino, M.D., Bazzano, G., Cisbani, E., De Angelis, C., Esposito, G., Limosani, F., Nenzi, P., Nigro, V., Ronsivalle, C., Santavenere, F., Surrenti, V., Trinca, E., Vincenti, M.A., Montereali, R. M., 2025b. Energy spectrum of protons below 10 MeV using color-center radiophotoluminescence in LiF crystals: a Monte Carlo-supported random-optimization estimator. Nucl. Instrum. Methods Phys. Res. 1072, 170218.

Palik, E.D., 1991. Handbook of Optical Constants of Solids II. Academic Press, San Diego, CA.

Picardi, L., Ampollini, A., Bazzano, G., Cisbani, E., Ghio, F., Montereali, R.M., Nenzi, P., Piccinini, M., Ronsivalle, C., Santavenere, F., Surrenti, V., Trinca, E., Vadrucci, M., Wembe Tafo, E., 2020. Beam commissioning of the 35 MeV section in an intensity modulated proton linear accelerator for proton therapy. Phys. Rev. Accel. Beams 23, 020102.

Piccinini, M., Ambrosini, F., Ampollini, A., Carpanese, M., Picardi, L., Ronsivalle, C., Bonfigli, F., Libera, S., Vincenti, M.A., Montereali, R.M., 2014. Solid state detectors based on point defects in lithium fluoride for advanced proton beam diagnostics. J. Lumin. 156, 170.

Piccinini, M., Ambrosini, F., Ampollini, A., Picardi, L., Ronsivalle, C., Bonfigli, F., Libera, S., Nichelatti, E., Vincenti, M.A., Montereali, R.M., 2015. Photoluminescence of radiation-induced color centers in lithium fluoride thin films for advanced diagnostics of proton beams. Appl. Phys. Lett. 106, 261108.

Piccinini, M., Nichelatti, E., Ampollini, A., Picardi, L., Ronsivalle, C., Bonfigli, F., Libera, S., Vincenti, M.A., Montereali, R.M., 2017. Proton beam dose-mapping via color centers in LiF thin film detectors by fluorescence microscopy. Europhys. Lett. 117, 37004.

Piccinini, M., Nichelatti, E., Ronsivalle, C., Ampollini, A., Bazzano, G., Bonfigli, F., Nenzi, P., Surrenti, V., Trinca, E., Vadrucci, M., Vincenti, M.A., Picardi, L., Montereali, R.M., 2019. Visible photoluminescence of color centers in LiF crystals for advanced characterization of 18 – 27 MeV proton beams in a wide fluence range. Radiat. Meas. 124, 59.

Piccinini, M., Nichelatti, E., Pimpinella, M., De Coste, V., Montereali, R.M., 2022. *Dose response of visible color center radiophotoluminescence in lithium fluoride crystals irradiated with a reference ^{60}Co gamma beam in the 1–20 Gy dose range.* Radiat. Meas. 151, 106705.

Piccinini, M., Nichelatti, E., Vincenti, M.A., Nigro, V., Ronsivalle, C., Ampollini, A., Nenzi, P., Bazzano, G., Tinca, E., Montereali, R.M., 2023. Dynamic range and dose linearity of the radiophotoluminescence intensity in lithium fluoride crystals irradiated with 2.3 and 26 MeV protons. J. Lumin. 259, 119833.

Piccinini, M., Mirandola, A., Nigro, V., Vincenti, M.A., Ciocca, M., Montereali, R.M., 2024a. Radiophotoluminescence response of LiF:Mg,Ti pellets irradiated with clinical proton beams in the 70-200 MeV energy range. Radiat. Meas. 174, 107153.

Piccinini, M., Nichelatti, E., Esposito, G., Cisbani, E., Nigro, V., Vincenti, M.A., Limosani, F., Ronsivalle, C., Ampollini, A., De Angelis, C., Montereali, R.M., 2024b. Detection of fluorescent low-energy proton tracks in lithium fluoride crystals. Radiat. Meas. 174, 206701.

Piccinini, M., Nichelatti, E., Nigro, V., Menchini, F., Montecchi, M., Montereali, R.M., Ampollini, A., Ronsivalle, C., Vincenti, M.A., 2025. Detection of fluorescent low-energy proton tracks in lithium fluoride thin films on silicon substrates. J. Lumin. 287, 121496.

Sankowska, M., Bilski, P., Marczewska, B., 2022. Thermal enhancement of the intensity of fluorescent nuclear tracks in lithium fluoride crystals. Radiat. Meas. 157, 106845.

Schulman, J.H., Compton, W.D., 1963. Color Centers in Solids. Pergamon Press, Oxford, UK, p. 331. Ch. XI.

Sharopov, U., Juraev, T., Kakhkhorov, S., Juraev, K., Kurbanov, M., Karimov, M., Saidov, D., Kakhramonov, A., Akbarova, F., Rakhmatshoev, I., Abdurakhmonov, O., 2025. New challenges for lithium fluoride: from dosimeter to solid-state batteries. Next Mater. 8, 100548 (review).

The MathWorks, Inc., 2010. Matlab V. 7.10.0 (R2010A). Natick, MA.

Villarreal-Barajas, J.E., Piccinini, M., Vincenti, M.A., Bonfigli, F., Khan, R., Montereali, R. M., 2015. Visible photoluminescence of colour centres in LiF crystals for absorbed dose evaluation in clinical dosimetry. IOP Conf. Ser. Mater. Sci. Eng. 80, 12020.

Vincenti, M.A., Leoncini, M., Libera, S., Ampollini, A., Mancini, A., Nichelatti, E., Nigro, V., Picardi, L., Piccinini, M., Ronsivalle, C., Rufoloni, A., Montereali, R.M., 2021. Enhanced F_2 and F_3^+ colour centres photoluminescence response of LiF film-based detectors for proton beams. Opt. Mater. 119, 111376.

Vincenti, M.A., Nichelatti, E., Nigro, V., Piccinini, M., Albertazzi, B., Benkadoum, Y., Dabrowski, H., Koenig, M., Rigon, G., Mabey, P., Mercere, P., Da Silva, P., Pikuz, T., Ozaki, N., Filippov, E., Makarov, S., Pikuz, S., Montereali, R.M., 2023. Visible radiophotoluminescence of color centers in lithium fluoride thin films for high spatial resolution imaging detectors for hard X-rays. ECS J. Solid State Sci. Technol. 12, 066008.

Website. https://fluka.cern.